QUANTUM CHAOS AND MESOSCOPIC SYSTEMS

Final Technical Report

by

Giulio Casati: Principal Investigator

July 1997

United States Army

EUROPEAN RESEARCH OFFICE OF THE U.S. ARMY

London, England

CONTRACT NUMBER **N68171-96-C-9039**

Centro di Cultura Scientifica "A. Volta"

Villa Olmo - 22100 Como - Italy

REPORT DOCUMENTATION PAGE

Form Approved
OMB No. 0704-0188

1. AGENCY USE ONLY (Leave blank)	2. REPORT DATE	3. REPORT TYPE AND DATES COVERED
	June 1997	Final Report January-March 1997

4. TITLE AND SUBTITLE
Quantum Chaos and Mesoscopic Systems

5. FUNDING NUMBERS
N68171-96-C-9039
Rod 7582-EE-01

6. AUTHOR(S)
Giulio Casati
Italo Guarneri

7. PERFORMING ORGANIZATION NAME(S) AND ADDRESS(ES)
Centro di Cultura Scientifica "A. Volta"
Villa Olmo, Via Cantoni, 1 - 22100 Como, Italy
Centro Sistemi Dinamici
Via Lucini, 3 - 22100 Como, Italy

8. PERFORMING ORGANIZATION REPORT NUMBER
DYSCO 79

9. SPONSORING/MONITORING AGENCY NAME(S) AND ADDRESS(ES)

10. SPONSORING/MONITORING AGENCY REPORT NUMBER

11. SUPPLEMENTARY NOTES

12a. DISTRIBUTION/AVAILABILITY STATEMENT

DISTRIBUTION STATEMENT A
Approved for public release
Distribution Unlimited

12b. DISTRIBUTION CODE

13. ABSTRACT (Maximum 200 words)

The interplay of classical chaotic properties and of quantum coherence effects is crucially important in mesoscopic physics, as it gives rise to transport fluctuations and quantum localization. We have studied both effects in different models. The results we have obtained are potentially relevant to all fields of Quantum Chaology, with possible experimental applications in the domains of Atomic Physics, Mesoscopic Physics, and Classical wave propagation (e.g. acoustic, microwave and optical resonators).

14. SUBJECT TERMS	15. NUMBER OF PAGES
	21
	16. PRICE CODE

17. SECURITY CLASSIFICATION OF REPORT	18. SECURITY CLASSIFICATION OF THIS PAGE	19. SECURITY CLASSIFICATION OF ABSTRACT	20. LIMITATION OF ABSTRACT

NSN 7540-01-280-5500

Standard Form 298 (Rev. 2-89)
Prescribed by ANSI Std. Z39-18
298-102

ATTACHMENT 1
PAGE 1 OF 2

Table of Contents

Abstract

The interplay of classical chaotic properties and of quantum coherence effects is crucially important in mesoscopic physics, as it gives rise to transport fluctuations and quantum localization. We have studied both effects in different models. Concerning conductance fluctuations in mesoscopic devices, we have exploited a Band Random Matrix model to investigate the lively debated question, of the connection between the different definitions of conductance, which are due to Thouless and Landauer, respectively. We have found that they coincide, apart from a numerical factor, in the metallic regime, but not in the insulator one, where they scale differently with the sample length.

Concerning localization, we have found evidence that this phenomenon - hitherto known for electrons in disordered solids, or for externally driven systems - is instead a much more general occurrence in the quantal dynamics of chaotic systems. We have studied the classical and quantum dynamics of a billiard, which is chaotic in the classical limit, and which is accessible to experimental investigation. We have found evidence for a quantum localization effect, which sets some limitations to the applicability of Random Matrix theory, and we have given quantitative conditions for that.

These results are potentially relevant to all fields of Quantum Chaology, with possible experimental applications in the domains of Atomic Physics, Mesoscopic Physics, and Classical wave propagation (e.g., acoustic, microwave and optical resonators).

1 Background

Quantum chaology is the area of theoretical physics which is concerned with the investigation of the properties of quantum systems which are chaotic in the classical limit[1][2]. It was started as a highly theoretical subject, but has recently come closer to direct physical applications thanks to developments in the field of Mesoscopic Physics [3]. This name describes submicron-size systems in which electrons behave quite differently than in atoms, which are much smaller, or in macroscopic solid samples, which are much larger. Typical examples are conductor or semiconductor devices (e.g., transistors) of a few thousand angstroms, which behave in a peculiar way due to quantum coherence effects; for example, they exhibit Mesoscopic Fluctuations.

The fast progress of microelectronics in manifacturing devices of very small size makes the understanding of such phenomena a very important task not only for theoretical physics but also for technology.

Viewed from the standpoint of Classical Mechanics, the electronic dynamics relevant to mesoscopic physics is usually chaotic. On the other hand, quantum coherence is extremely important on the mesoscopic scale, so that the behaviour of mesoscopic systems is actually dominated by quantum effects. The combination of classical chaotic dynamics and quantum coherence has phenomenological manifestations in the form of localization effects, and of fluctuations of transport coefficients. Localization and transport fluctuations are therefore a major feature of mesoscopic physics, and their study is a primary theoretical task, because they appear to be a rather general feature of quantum mechanics in the presence of classical chaos, and not just of particle motion in a disordered potential.

Classical chaotic systems exhibit fluctuations, which are not due to external random agents (such as noise, or thermal effects), but rather to uncontrollable, small variations in the preparation of the state, which are rapidly amplified by the dynamics. On the other hand, quantum systems exhibit specific quantum fluctuations, which are not due to any such effect but are intrinsic to the very concept of a quantum state. Such quantum fluctuations are washed out by the process of quantum averaging, which produces expectation values that are usually dynamically stable. There are, however, cases in which even quantum averages themselves fluctuate: such fluctuations have a dynamical origin, and are presumably connected to classical chaotic fluctuations.

Phenomenologically relevant instances are well known from several fields. Mesoscopic conductance fluctuations of small metallic samples at low temperature are a very popular example[3]. Great progress has been made possible in the study of such fluctuations by the use of Random Matrix Theory, which approaches the study of some relevant properties starting from the assumption that quantum Hamiltonians or Scattering Matrices can be written as matrices with randomly generated elements.

The primary objects of interest in the Random Matrix theoretical approach are the statistical properties of the energy spectrum, which describe how are the eigenvalues distributed, and their sensitivity to changes in external parameters, such as, e.g., external magnetic fields. In the RMT approach, a detailed description of the spectra is given up; only statistical features are considered. These turn out to be to some extent universal; in fact, their gross features are already reproduced if the Hamiltonian is replaced by a Random Matrix, i.e., by a matrix with randomly generated matrix elements, which does not retain any of the specific details of the original hamiltonian, other than its symmetry class .

According to current understanding, recourse to Random Matrix Theory is justified, when the system is quantally ergodic. By this one qualitatively means, that eigenstates are maximally extended over the whole energetically allowed energy range, in such a way as to give rise to phase-space distributions which fill the whole classically allowed energy shell. However, it is not by any means obvious that such a structure of eigenstates should be typical of systems which are strongly chaotic in the classical limit; in fact deviations from ergodicity may occur, due to several quantum effects.

The most important such effect is dynamical localization. This is an interference effect essentially similar to the Anderson localization which is undergone by quantum particles moving in a random potential. Anderson localization has a counterpart in the quantum dynamics of periodically driven systems[4], which is liable to experimental detection in atoms or molecules in external electromagnetic fields[5][6]. Dynamical localization results in strongly nonergodic eigenstates, and severely affects quantum transport, either in configuration, or in momentum space, or in both; in addition, it leads to statistical properties of energy spectra, quite at variance with Random Matrix predictions.

2 Statement of Problems.

As discussed above, transport fluctuations and localization are extremely important issues in Mesoscopic Physics, and their study was the main goal of the work summarized in this report.

2.1 Transport Fluctuations

There are two theoretical approaches to the definition of the conductance of a mesoscopic system, due to Thouless and Landauer respectively. They will be reviewed in the following section. The connection between these different definitions is a theoretically intricate problem, as yet not completely solved.

In Thouless' definition, a metallic sample is considered to be a closed system, and the effect of the external world is embodied in the boundary conditions to which the electronic wave function is subjected. Conductance is then related to the sensitivity of eigenvalues to changes in the boundary conditions.

In contrast, in the Landauer approach, the metallic sample is an open system, coupled to perfect conductors which carry electronic waves; these are partly transmitted and partly reflected by the sample. Conductance is then related to the transmission coefficient, obtained from the scattering matrix.

A special kind of Random Matrices, characterized by a band structure ("Band Random Matrices", BRM) , provides an efficient model for investigating the connection between the two definitions. Such matrices have been rather poorly investigated until recently, and are in a sense intermediate between the conventionally used Random Matrices, whose essential shortcoming is the lack of a meaningful classical limit, and the dynamical models of Quantum Chaos, which are endowed with such a limit but are more difficult to analyze.

Band Random Matrices exhibit a rich variety of statistical behaviours, depending on the values of a few characteristic parameters[7]. Different parameter ranges give rise to several different statistical regimes. In studying conductance through a disordered wire, one can model the Hamiltonian of electrons inside the wire by a BRM. If the wire is considered to be a closed system, boundary conditions have to be given; this is done by specifying φ, the fixed phase change prescribed on the wave function from one endpoint to

the other of the conducting sample. φ appears in the hamiltonian matrix as a phase, on which the matrix itself is periodically dependent; the sensitivity of eigenvalues to changes of this phase is then directly related to conductance by the famous Thouless formula:

$$g = \frac{1}{\Delta} \left\langle \left| \frac{\partial^2 E}{\partial \varphi^2} \right|_{\varphi=0} \right\rangle$$

where E is an eigenvalue, Δ is the average level spacing and $\langle . \rangle$ denotes average over disorder; g is the disorder-averaged dimensionless conductance.

2.2 Localization in Conservative systems

One of the main modifications that quantum mechanics introduces in the classical picture of chaotic dynamics is "quantum dynamical localization" which results e.g. in the suppression of chaotic diffusive-like process which may take place in systems under external periodic perturbations. This phenomenon, first pointed out in the model of quantum kicked rotator [10], is now firmly established and observed in several laboratory experiments [11].

How general is localization in the quantum mechanics of chaotic systems? For conservative Hamiltonian systems this question is but poorly investigated. The situation here is much more intriguing : from one hand, in a conservative system, one may argue that there is always localization due to the finite number of unperturbed basis states effectively coupled by the perturbation; on the other hand a large amount of numerical evidence indicates that quantization of classically chaotic systems leads to results which appear in agreement with the predictions of Random Matrix Theory (RMT)[12], and thus appears to exclude localization effects, because the latter would enforce deviations from RMT.

In previous works of ours[13] the problem of localization in conservative systems has been explicitely investigated. In particular, on the base of Wigner band random matrix model, conditions for localization were explicitely given, together with the relation between localization and level spacing distribution [14].

This is however an abstract result, because the extent to which the Wigner model reproduces the behaviour of actual quantum systems is not precisely known. One therefore needs to study more realistic models of chaotic sys-

tems, to check whether the prediction of localization in conservative systems which was obtained from the analysis of the Wigner model is actually valid.

Such models are provided, e.g., by billiards, which are very important in the study of chaotic conservative dynamical systems; in fact they are clear, mathematically well understood examples of classical chaos, and their quantum properties have been extensively studied theoretically and experimentally. Semiconductor devices in which electrons are subject to billiard-like dynamics have been fabricated; moreover, billiards are becoming increasingly relevant for the study of optical processes in microcavities, which may lead to possible applications such as the design of novel microlasers or other optical devices [15].

We have focused our attention on a well-known two dimensional chaotic billiard: the Bunimovich stadium, and have analyzed the conditions for quantum localization and therefore the conditions under which the standard Random Matrix Theory is not applicable.

3 Results: qualitative Summary.

Our work on quantum transport in mesoscopic conductors was aimed at clarifying the lively debated problem of the connection between different definitions of conductance of metallic samples of mesoscopic size. Having numerically computed conductance according to both definition, we found that they behave differently in the Ohmic and in the insulator regime. The difference between these regimes is set by the localization effect, and quantitatively measured by the localization ratio, i.e. the ratio between the localization length and the size of the sample. When this ratio is large, localization effects are negligible, and conductance scales inversely proportional to the sample length, according to Ohm's law. In this regime the two definitions of conductance yield essentially the same result, apart from a proportionality factor.

In contrast, when the localization ratio is small, the conductance decreases exponentially fast when the sample length is increased. Here the Thouless and the Landauer conductance are quite different, one of them scaling approximately like the square of the other.

The other question we have analyzed is, how general is localization in quantum chaotic systems? To this end we have studied the Bunimovich

stadium, a billiard which is well-known to be chaotic in the classical limit we have been able to show that quantum localization, until now believed to appear only in disordered or in externally driven systems, is also present in conservative systems such as billiards, and imposes certain limitations on the applicability of Random Matrix theory.

Notice that the effect predicted here is entirely due to quantum dynamical localization, and bears no relation with other, frequently considered, but much less generic, sources of deviations from RMT; for example, the existence of bouncing ball orbits. The same behaviour will in fact be present in chaotic billiards in which no family of periodic orbits exists.

The effects of quantum localization discussed here should be observable in microwave or sound wave experiment. We also would like to mention that the diffusive process in angular momentum and the corresponding suppression caused by quantum mechanics may be of interest for a new class of optical resonators which have been recently proposed [15].

4 Results: technical description.

4.1 Transport fluctations.

In our model the electron dynamics in the leads is described by two semi-infinite BRM's with the same bandwidth b, with all matrix elements inside the band equal to 1. The Schrödinger equation is

$$\sum_{k=-(b+1)}^{b+1} h_{i,i+k} u_{i+k} = E u_i \tag{1}$$

where $h_{i,j}$ are the non zero elements of the Hamiltonian H. Then, we can write $H = H_0 + V$, where H_0 is a BRM of the same rank of H and with the same band width, but with all non zero elements equal to 1; this decomposition defines the potential V of the scattering problem. Free waves in the leads (which are solutions of (1) with $h_{ij} = 1$ inside the band) are of the form $u_m = \frac{1}{\sqrt{2\pi}} e^{-ikm}$, with the wave number k obeying the dispersion law

$$\frac{\sin\left(\frac{2b+1}{2}k\right)}{\sin\left(\frac{k}{2}\right)} = E. \tag{2}$$

The left hand side of (2) is a periodic function of period 2π, which takes the value $2b+1$ when its argument is a multiple of 2π. Eq.(2) has always $2b$ solutions for $-1 < E < +1$, which can be found analytically for $E = 1$, $E = 0$ and $E = -1$ or with any required precision by numerical methods at any other value of E. For example, they are $k_j = \frac{2\pi j}{2b+1}$ with $j = 1 \cdots 2b$ for $E = 0$ and $k_s = \frac{2\pi s}{b}$ with $s = 1 \cdots b-1$ and $k_t = \frac{2\pi t+\pi}{b+1}$ with $t = 0 \cdots b$ for $E = 1$. The various allowed values of the wave-number k at a given energy E correspond to different scattering channels. We have thus a multi-channel scattering problem with exactly b ingoing and b outgoing channels, which, if $1 << b << L$, formally reproduces the case of a quasi-one dimensional wire.

The scattering properties of the conductor are described by a unitary scattering matrix S, that relates incoming and outgoing amplitudes, $I_{L(R)}$ and $O_{L(R)}$:

$$S \begin{pmatrix} I_L \\ I_R \end{pmatrix} = \begin{pmatrix} O_L \\ O_R \end{pmatrix} \tag{3}$$

where the subscripts L and R stand for the left and the right lead. The S matrix can be written as

$$S = \begin{bmatrix} r & t \\ t' & r' \end{bmatrix} \tag{4}$$

where t and t' are the transmission sub-matrices in the two opposite directions, and r and r' are the reflection sub-matrices.

The Landauer conductance is given by

$$\mathcal{G} = \frac{e^2}{2\pi\hbar} \sum_{ij} |t_{ij}|^2, \tag{5}$$

where t_{ij} are the elements of the t sub-matrix. We have computed the S-matrix by standard methods, by numerically solving the Lippman-Schwinger equation

$$u^{\pm} - G_0^{\pm} \cdot V u^{\pm} = u \tag{6}$$

where u are free eigenfunctions, $u^{\pm}$ interacting ones, and the potential V is the difference between the interacting Hamiltonian and the free one. The free Green function, $G_0^{\pm} = (E - H_0 \pm i\epsilon)^{-1}_{\epsilon=0}$, has matrix elements

$$(G_0^{\pm})_{n,m} = \langle n|(E - H_0 \pm i\epsilon)^{-1}|m\rangle|_{\epsilon=0}$$

$$= \frac{1}{2\pi} \int_0^{2\pi} dk \frac{e^{-i(m-n)k}}{E \pm i\epsilon - \frac{\sin(\frac{2b+1}{2}k)}{\sin(\frac{k}{2})}} \Bigg|_{\epsilon=0}$$

that were numerically computed by exploiting the Theorem of Residues. Finally, the scattering matrix was computed via the usual formula:

$$S_{ij} = \delta_{ij} - 2\pi \sqrt{\frac{dk_i}{dH}}\Bigg|_{H=E} \sqrt{\frac{dk_j}{dH}}\Bigg|_{H=E} < u_i \,|V|\, u_j^{\pm} > \tag{7}$$

The unitarity condition $S^+S = 1$ provides a check on the precision of the results, and was fulfilled within a typical error 10^{-10}.

We have considered the dimensionless residual conductance

$$g = \frac{2\pi\hbar}{e^2}\mathcal{G} \tag{8}$$

and investigated the scaling properties of the geometric average $g_{av} = \exp\overline{\langle \ln g \rangle}$ in the regime $1 \ll b \ll L$, where L is the length of the disordered sample. The brackets $\langle\rangle$ mean here average over different realizations of the potential (1000 realizations in our computations) while the bar means average over the energy range $(-1, 1)$. As expected, g_{av} turned out to depend on b and L only through the localization parameter $x = \frac{b^2}{L}$ (Fig.1). For $x \gg 1$, i.e. in the delocalised regime, this dependence has the form $g_{av} \propto x \propto L^{-1}$, which is the "ohmic" behavior (Fig. 2). Instead, in the localised regime $x \ll 1$, $g_{av} \approx \exp(-c/x)$ (Fig. 3).

Our results can be summarized by the following interpolating law, valid in all regimes:

$$g_{av} = \frac{a + b\exp(-d/x)}{\exp(c/x) - 1} \tag{9}$$

where $c \approx 2.70$ and $d \approx 0.55$ (obtained from the fitting in the localised region) and $a \approx 6.58$ and $b \approx -5.53$ (obtained from the fitting in the metallic region). If the conductance is computed without performing the energy average, a similar scaling law is obtained, though with slightly different constants (curves **a** and **b** in Fig. 4).

We turn now to the Thouless approach. In order to define the (dimensionless) Thouless conductance, the BRM which describes the disordered sample has to be 'periodicized'. The 'periodic' BRM thus obtained describes a ring-shaped conductor, and depends on a phase ϕ that has the meaning of an

Aharonov-Bohm flux switched on through the ring. The disorder-averaged Thouless conductance is

$$\mathcal{K} = \frac{1}{\Delta} \left\langle \left| \frac{d^2 E}{d\varphi^2} \right| \Big|_{\varphi=0} \right\rangle \tag{10}$$

where Δ is the mean level spacing, and $\langle\rangle$ denotes statistical averaging. The scaling properties of $\mathcal{K}$ were analyzed in detail in ref.([7]), which is the source of the data used below. In that work, the eigenvalues sequence was unfolded to have unit density, so that $\mathcal{K} = K_{av} = \exp\langle \ln K \rangle$, where $K = |E''(0)|$. The numerical data show that Thouless conductance obey the same scaling (9), but with constants $a' \approx 0112$, $b' \approx -3.12310^{-2}$, $c' \approx 1.565$ and $d' \approx 0.989$.

One key problem in comparing the Thouless and the Landauer conductance is connected with the matching of the "free" and of the "disordered" part of the Hamiltonian, i.e., with the effect of "contacts", which was discussed in refs.[8]. If the arbitrary scale factor α appearing in the disordered part of our hamiltonian is varied, while keeping the free hamiltonian unchanged, the Thouless conductance is not by any means affected, nor is the value of the localization length in the 'infinite' sample. The Landauer conductance, instead, is to some extent modified. It becomes very small both at small and at large values of α, and it has a relatively broad maximum around $\alpha = 1$. A value of α close to 1 is also found on requiring that the local density of states for the "free" dynamics is the same as the density of interacting states in the sample (having computed the latter from the interacting Green function, in a standard way). Our choice of $\alpha = 1$, which maximizes the transmission, is very similar to the "matching wire" prescription, suggested by Economou and Soukoulis.

The comparison between Landauer and Thouless conductance, computed as described above, is shown in Fig.4. In particular, in the metallic regime ($x \gg 1$) we have $g_{av} \approx (7.5 \pm 0.4) K_{av} + 0.8$, namely the two conductances are proportional in the diffusive region, where (10) is assumed to be valid. The meaning of the coefficent of proportionality $\approx 7.5 \pm 0.4$ is not clear to us. It is of course possible that this coefficient becomes closer to 1 in the limit $b \to \infty, L \to \infty, b^2/L = const.$; this we were unable to check due to obvious numerical limitations, but, in the parameter range we were able to explore, the variation of this factor is quite slight.

In the localised regime ($x \ll 1$) we get $\ln(g_{av}) \approx (1.73 \pm 0.09) \ln(K_{av}) + 5.66$, that to say, the Landauer conductance is proportional to K_{av}^{β}, with

$\beta = 1.73 \pm 0.09$. The large error in this numerical estimate is due to the difficulty to compute curvatures in the localised regime. In this connection, we have also studied two different tridiagonal models: a BRM with $b = 1$ and an Anderson model with Gaussian disorder on the main diagonal. Comparing Landauer conductance and curvature on these two models we got $\beta_{BRM} = 2.078 \pm 0.036$ and $\beta_{And} = 2.088 \pm 0.005$l. It seems therefore reasonable to conjecture $\beta = 2$; it is also worth mentioning that theoretical arguments suggest that the dissipative conductance is proportional to the squared curvature in the deeply localised regime[9].

4.2 Localization in billiards.

We consider the motion of a particle having mass m, velocity $\vec{v}$ and elastically bouncing inside the stadium shown in Fig 5. We denote with R the radius of the semicircles and with $2a$ the length of the straight segments. The total energy is $E = m\vec{v}^2/2$. The statistical properties of the billiard are controlled by the dimensionless parameter $\epsilon = a/R$ and, for any $\epsilon > 0$, the motion is ergodic, mixing and exponentially unstable with Lyapunov exponent Λ which, for small ϵ, is given by [16] $\Lambda \sim \epsilon^{1/2}$.

For the analysis of classical dynamics, a typical choice of canonical variables is (s, v_t) where s measures the position along the boundary of the collision point and v_t is the tangent velocity. These variables however, are quite difficult to treat from the quantum point of view. For this purpose it is convenient instead to consider l, the angular momentum calculated with respect to the center of the stadium, and the angle θ which describes, together with $r(\theta)$, the position of the particle in the usual polar coordinates. It is important to stress that with this choice of variables, the invariant measure $d\mu = dsdv_t$ is preserved only to order ϵ, that is $d\mu = dsdv_t = d\theta dl + o(\epsilon)$

At a given energy E, the angular momentum must satisfy the relation $|l| < l_{max} = (R + a)\sqrt{2Em}$. It is therefore convenient to introduce the rescaled quantity $L = l/l_{max}$. Then the classical motion takes place on the cylinder $0 \leq \theta < 2\pi$, $-1 < L < 1$.

It is expected that for $\epsilon << 1$ a diffusive process will take place in angular momentum with a diffusion coefficient $D = D(\epsilon)$. In order to obtain an estimate for $D(\epsilon)$ we now derive an explicit expression for the boundary map in the variables (L, θ). The change ΔL after a collision with the boundary can be easily obtained to order ϵ, by neglecting collisions with straight lines

and by taking into account that in the collision only the normal velocity $v_n = \vec{v} \cdot \vec{n}$ changes the sign. Here $\vec{n} \simeq \vec{e}_r + \epsilon \sin\theta sign(\cos\theta)\vec{e}_\theta$, $\vec{e}_r$ and $\vec{e}_\theta$ being the usual polar coordinates unit vectors. One then get :

$$\Delta L = \bar{L} - L = -2\epsilon \sin\theta sign(\cos\theta) sign(L)\sqrt{1 - L^2} \tag{11}$$

On the other side the change in θ, to zero order, is given by :

$$\Delta\theta = \bar{\theta} - \theta = \pi - 2\arcsin(\bar{L}) \tag{12}$$

According to a standard procedure [17] we introduce a generating function $G(\bar{L}, \theta)$ in such a way that the map defined by

$$L = \frac{\partial G}{\partial \theta}; \qquad \bar{\theta} = \frac{\partial G}{\partial \bar{L}} \tag{13}$$

coincides with ΔL at first order in ϵ and with $\Delta\theta$ at zero-th order. The generating function is given by:

$$G(\bar{L}, \theta) = (\theta + \pi)\bar{L} - 2\int^{\bar{L}} dL \arcsin L + \epsilon g(\bar{L})|\cos\theta| \tag{14}$$

where $g(\bar{L}) = 2sign(\bar{L})(1-\bar{L}^2)^{1/2}$. The generated (implicit) area–preserving map is

$$\begin{aligned} \bar{L} &= L - 2\epsilon \sin\theta sign(\cos\theta) sign(\bar{L})(1 - \bar{L}^2)^{1/2} \\ \bar{\theta} &= \theta + \pi - 2\arcsin(\bar{L}) + \epsilon g'(\bar{L})|\cos\theta| \end{aligned} \tag{15}$$

By taking the local approximation in the angular momentum, the map (15) writes :

$$\begin{aligned} \bar{L} &= L - 2\epsilon \sin\theta sign(\cos\theta) sign(\bar{L})\sqrt{1 - L_0^2} \\ \bar{\theta} &= \theta + \pi - 2\arcsin(\bar{L}) \end{aligned} \tag{16}$$

which remains area–preserving and can be easily iterated (here L_0 is the initial angular momentum).

The agreement of map (16) with the true dynamics can be numerically checked and it is shown in Fig.6 where we plot $L^* = (\bar{L} - L)/(2\epsilon\sqrt{1 - L_0^2})$ against θ. Points represent billiard dynamics while the full line is the function $f(\theta) = -\sin\theta sign(\cos\theta)$.

Notice that the function $f(\theta)$ is periodic of period π and has a discontinuity at $\theta = \pi/2$. This gives to the map (16) a structure very close to the sawtooth map which is known[18] to be chaotic and diffusive with a diffusion rate D which, for small values of the kick strength ϵ, is given by $D \sim \epsilon^{5/2}$. This behaviour, according also to our numerical computations, appears to be generic for maps which have such type of discontinuity.

We proceed now to a numerical investigation of the diffusive process. To this end we consider a distribution of particles with given initial L_0 and random phases θ in the interval $(0, 2\pi)$ and integrate the classical equations of motion inside the billiard. In Figs. 7a,b we present the behaviour of $\Delta L^2 = \langle L^2 \rangle - \langle L_0 \rangle^2$ as a function of the number of collisions n and the distribution function $f_n(L)$ at fixed n as a function of $(L - L_0)$. As it is seen, ΔL^2 grows diffusively and the distribution function is in good agreement with a Gaussian[1] . In particular the dependence $D = D(\epsilon)$ of the diffusion coefficient can be easily computed and the result $D = D_0 \epsilon^{5/2}$ (see Fig.8) is in agreement with predictions of map (16) with $D_0 = 1.5$.

The analysis of the classical diffusive process allows to make some predictions concerning the quantum motion and in particular to estimate the conditions under which the quantum localization phenomenon will take place [19]. First of all, in order that any quantum diffusive process may start it is necessary to be above the perturbative regime. In particular the level number must be sufficiently high so that the De Broglie wavenumber k of the corresponding wavefunction must satisfy the relation $k > 1/a$. This implies $E > E_p = \hbar^2/2ma^2$ which is the energy necessary to confine a quantum particle inside a box of length a. Using the well known Weyl formula for the total number of states with energy less than E [12]

$$\langle N(E) \rangle \approx \frac{m\mathcal{A}}{2\pi\hbar^2} E \approx \frac{1}{8} m \left(\frac{R}{\hbar}\right)^2 E \qquad (17)$$

where $\mathcal{A}$ is the area of a quarter of billiard, and keeping only the leading

[1]It may be interesting to remark that the diffusion coefficient computed in terms of the number of collisions, appears to depend on the initial value of angular momentum L. This is due to the fact that the mean free path depends on angular momentum and that even though the system is ergodic, ergodicity is not uniform in time. If one computes the diffusion coefficient in terms of real physical time then the dependence on the initial L_0 value disappears. For the above reasons map (6) approximate the real dynamics provided L_0 is not too close to 1.

term, we obtain that in order to be in a non perturbative regime we have to consider level numbers

$$N \gg N_p \simeq \frac{1}{16\epsilon^2} \tag{18}$$

We call N_p perturbative border.

According to the well known arguments [20], above the perturbative border (18) quantum diffusion in angular momentum takes place with a diffusion coefficient close to the classical one. This diffusion proceeds up to a time $\tau_B \sim D_{eff}/\hbar^2$ after which diffusion will be suppressed by quantum interference. This time is related to the uncertainty principle. Namely, for times less than τ_B the discrete spectrum is not resolved and the quantum motion mimics the classical diffusive motion [20, 21]. Here $D_{eff} = D_0\epsilon^{5/2}2mER^2$ is the classical diffusion coefficient in real (not scaled) angular momentum.

The nature of the quantum steady state will depend crucially on the ergodicity parameter [21]

$$\lambda^2 = \frac{\tau_B}{\tau_E} \tag{19}$$

where $\tau_E = l_{max}^2/D_{eff} \simeq 2mER^2/D_{eff}$ is the ergodic relaxation time.

For $\lambda \ll 1$ the quantum steady state is localized while for $\lambda \gg 1$ we have quantum ergodicity. The critical value $\lambda = 1$ leads to $l_{max}\hbar = D_{eff}$ that is $E = E_{erg} = \epsilon^{-5}D_0^{-2}\hbar^2/2mR^2$. We then have :

$$N = N_{erg} \simeq \frac{1}{16D_0^2\epsilon^5} \tag{20}$$

It follows that only for $N > N_{erg}$ there is quantum ergodicity and therefore one expects statistical properties of eigenvalues and eigenfunctions to be described by RMT. Instead for $N < N_{erg}$, even if $N \gg N_p$, namely very deep in quasiclassical regions, statistical properties will depend on parameter $\lambda = D_0\sqrt{8N\epsilon^5}$ and not separately on ϵ or N. For example, the nearest neighbour levels spacing distribution $P(s)$ will approach e^{-s} when $\lambda \ll 1$.

We have tested this prediction by numerically computing the level spacing distribution for different values of ϵ and N. One example is shown in Fig.9 for which $N \gg N_p$ but since $\lambda \ll 1$ the distribution $P(s)$ is close to e^{-s} as expected. Similar behaviour is expected for other quantities such as

the two points correlation function, the probability distribution of eigenfunctions, etc. The numerical computations are based on the improved plane wave decomposition method. The accuracy of eigenvalues is better than one percent of the mean level spacing. We also compared the results with the semiclassical formula in order to check that there are no missing levels.

5 Conclusions and Recommendations

In this report we have summarized the one-year work we have done in partial accomplishment of a three years research proposal. Results of this work appeared in papers[22][23].

In the study of electronic transport in mesoscopic conductors, conductance is the primary object of interest; still, from the theoretical viewpoint, it is defined in two different ways, which bear no obvious connection to each other, and we have supplied empirical evidence for the relationship between them.

The other theme of our investigation was localization. Contrary to general expectations, we have shown that this famous effect is not restricted to transport in disordered solids, but is instead a rather general occurrence when a chaotic system in which a classical diffusion occurs is quantized. This result has fundamental implications: first, it indicates certain limits to which the generally believed validity of Random Matrix Theory as a description of strongly chaotic systems is subject; second, it brings into light a quantal source of nonergodic behavior, which may have unexpected implications for quantum statistical mechanics.

The area explored in this research is potentially relevant to several fields of Physics, starting from those in which Random Matrix Theory is recognizedly a basic theoretical tool, and which include practically all the fields of Quantum Chaology, with direct physical applications to Atomic Physics, Disordered Solids, and Mesoscopic Physics.

Localization effects of the kind we have investigated are important also for many body systems, hence for Nuclear Physics. On a fundamental level, they directly affect the validity of the quasiclassical approximation, therefore their study is crucial in understanding the quantum-classical correspondence in general, and the mechanism of decoherence in particular. Finally, beyond quantum mechanics, they are also relevant to classical wave mechanics

(electromagnetic, elastic, light waves).

The methods involved in this investigation range from standard semiclassical methods, to field-theoretical methods (non-linear σ-model), to sophisticated techniques of numerical simulation.

On the level of experiments, several branches of experimental physics are involved, including nuclear physics, atomic physics, besides mesoscopic devices.

Figure Captions

Figure 1. Logarithm of the geometric average of the Landauer conductance $g_{av} = \exp\overline{\langle \ln(g) \rangle}$ vs. logarithm of the scaling parameter $x = b^2/L$. Numerical data (circles) correspond to different values of L and b in the ranges $25 \leq L \leq 400$,$5 \leq b \leq 79$. The full line gives the fitting law.

Figure 2. Geometrical average of Landauer conductance vs. the scaling parameter b^2/L in the delocalised regime $b^2 >> L$; the linear fit shows the Ohmic behaviour of Landauer conductance.

Figure 3. $\ln(g_{av})$ vs. the inverse of the scaling parameter in the localised regime $b^2 << L$. The linear fit shows the exponential decrease of the Landauer conductance due to localization: $\overline{\langle \ln(g) \rangle} = -CL/b^2 + D$, with $C = 2.7 \pm 0.04$,$D = 1.9 \pm 0.2$.

Figure 4. Comparison between the fittings of Landauer conductance, computed with (curve a) and without (curve b) energy average in the interval $(-1, 1)$. Curve c shows the fit of the Thouless conductance computed in ref.[19].

Figure 5. The Bunimovich stadium with radius R and straight segments $2a$; the variables $(r(\theta), \theta)$ indicate the position of the point along the boundary.

Figure 6. Comparison between the billiard dynamics and the map (16). Here we plot the variable L^* versus θ (see text). Points are obtained from numerically integrating the motion of one particle in the billiard for 100 iterations, starting from $L_0 = 0$ and a random position along the boundary, while the full line is the function $f(\theta)$ (see text). Here $\epsilon = 0.01$. The points not belonging to the curve are due to collisions with one of the straight lines; this occurrence is outside the approximation of map (16).

Figure 7. Diffusion in angular momentum for the billiard with $\epsilon = 0.01$. Here an ensemble of 10^4 particles was chosen with initial $L_0 = 0$ and random position along the boundary. a) ΔL^2 as a function of the number of collisions

n; the dashed line is the best fit and gives $D = \Delta L^2/n = 1.5 \cdot \quad 10^{-5}$. b) Distribution function after $n = 500$ collisions averaged over the last 50 collisions. The full line is the best fitting Gaussian with average -0.016 and variance 0.1.

Figure 8. Diffusion coefficient $D = \Delta L^2/n$ for the stadium (full circles) as a function of ϵ. Open circles indicate the diffusion rate obtained from the map (6). The line is obtained by the usual best fitting procedure to the true dynamics (full circles) and gives $D = D_0\epsilon^{2.5}$ with $D_0 = 1.5$.

Figure 9. Level spacings distribution computed on 2000 levels in the interval $51000 < N < 53000$ for $\epsilon = 0.01$ (a) and $\epsilon = 0.1$ (b). In the first case (a) $N_p \simeq 600$ and $N_{erg.} \simeq 2.8 \cdot 10^8$ and therefore $N_p \ll N \ll N_{erg}$. The value $\lambda \simeq 0.01$ of the ergodicity parameter accounts for the fact that the numerically computed $P(s)$ is close to e^{-s} (full curve). In the case (b) one has $N_{erg} \simeq 2.8 \cdot 10^3 \ll N$ and therefore, as expected, the distribution $P(s)$ is close to Wigner-Dyson (dotted curve).

References

[1] M.C.Gutzwiller, *Chaos in Classical and Quantum Mechanics*, Springer, New York, 1990.

[2] M.V.Berry, Proc.R.Soc. London A, **400** (1985) 229.

[3] B.L.Altshuler and B.D.Simons, in *Proceedings of Les Houches Summer School, Session LXI, Mesoscopic Quantum Physics,* (1994) edited by E.Akkermans, G.Montambaux, J.L.Pichard and J.Zinn-Justin, North Holland, Amsterdam, 1995.

[4] S.Fishman, in *Quantum Chaos*, Proc. Int. School of Physics "Enrico Fermi", course CXIX (North-Holland 1994).

[5] F.L.Moore, S.C.Robinson, C.Bharucha, P.E.Williams, and M.Raizen, *Phys.Rev.Lett.* **73** (1994) 2974.

[6] J.Bayfield, G.Casati, I.Guarneri and W.Sokol, *Phys.Rev.Lett.* **63** (1989) 364.

[7] G.Casati, I.Guarneri, F:M:Izrailev, L.Molinari and K.Zyczkowski, *Phys. Rev. Lett.* **72** (1994) 2697.

[8] S.Iida, H.A.Weidenmuller and J.A.Zuk, *Ann. Phys. (NY)*, **200** (1990) 219.

[9] E.Akkermans, private communication.

[10] G.Casati, B.V.Chirikov, J.Ford and F.M.Izrailev, Lectures Notes in Physics **93** (1979) 33, Springer Verlag (see also Ref. 12).

[11] E. J. Galvez, B. E. Sauer, L. Moorman, P. M. Koch and D. Richards, Phys. Rev. Lett. **61**, (1988) 2011; J.E.Bayfield, G.Casati, I.Guarneri and D.Sokol Phys. Rev. Lett. **63**, (1989) 364; M.Arndt, A.Buchleitner, R.N.Mantegna, H.Walther Phys. Rev. Lett. **67**, (1991) 2435; F.L.Moore, J.C. Robinson, C.F.Bharucha, B.Sundaram and M.G.Raizen Phys. Rev. Lett. **75**, (1995) 4598.

[12] O.Bohigas, *Proceedings of the 1989 Les Houches Summer School on "Chaos and Quantum Physics"*, ed. M.J.Giannoni, A.Voros and J.Zinn-Justin, p.89, Elsevier Science Publisher B.V., North–Holland, (1991)

[13] G.Casati, B.V.Chirikov, I.Guarneri and F.Izrailev, Phisics Lett. **A23** (1996) 430.

[14] G.Casati, B.V.Chirikov, I.Guarneri and F.M.Izrailev Phys.Rev.E **48**, (1993) R1613; G.Casati, B.V.Chirikov, I.Guarneri and F.M.Izrailev preprint Budker INP 95-98 Novosibirsk, (1995).

[15] J.U.Nockel and A. D. Stone in *Optical Processes in Microcavities*, edited by R. K. Chang and A. J. Campillo (World Scientific Publishing Co., 1995), and A.Mekis, J.U.Nöckel, G.Chen, A.D.Stone and R.K.Chang, Phys. Rev. Lett. **75**, (1995) 2682. In these papers it is proposed that the spoiling of high-Q whispering gallery modes in deformed dielectric spheres can be understood as a transition to chaotic ray dynamics (in deformed circular billiards) which can no longer be confined by total internal reflection.

[16] G.Benettin, Physica **13D**, (1984) 211.

[17] A.J.Lichtenberg and M.A.Lieberman, *Regular and Stochastic Motion*, Applied Math. Series 38 (1983).

[18] I.Dana, N.W.Murray and I.C.Percival Phys.Rev.Lett. **62** (1989) 233.

[19] B.V.Chirikov preprint 90-116 Novosibirsk, (1990).

[20] B.V.Chirikov, F.M.Izrailev and D.L.Shepelyansky, Sov. Scient. Rev. **2C**, 209 (1981).

[21] G.Casati and B.V.Chirikov , "*Quantum Chaos*", Cambridge University press, (1995); Physica D, **86** (1995) 220.

[22] F.Borgonovi, G.Casati and Baowen-li, Phys.Rev.Lett. **77** (1996) 430.

[23] G.Casati, G.Maspero and I.Guarneri, to appear in J.Phys. (France) (1997)

Fig. 1

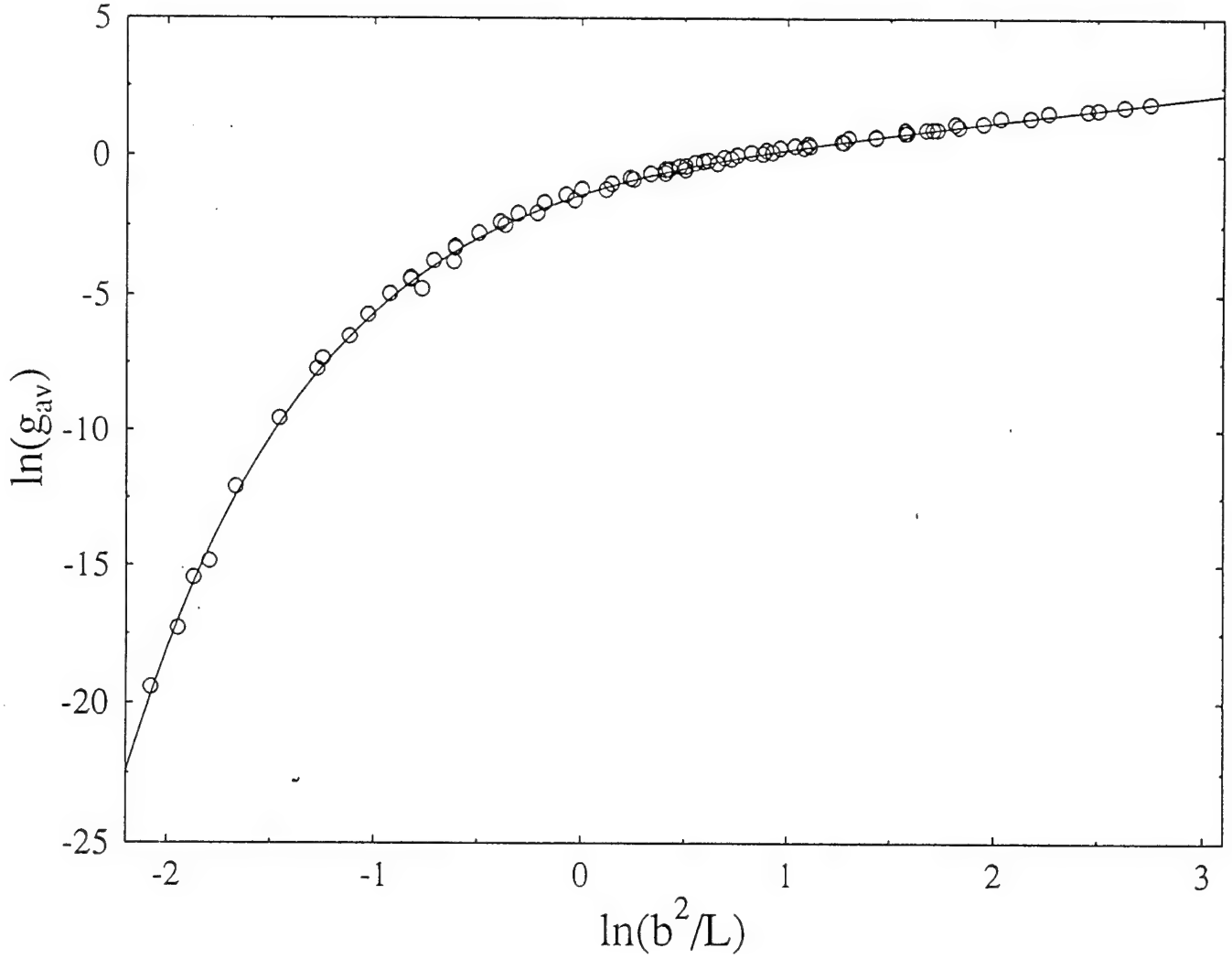

Fig. 2

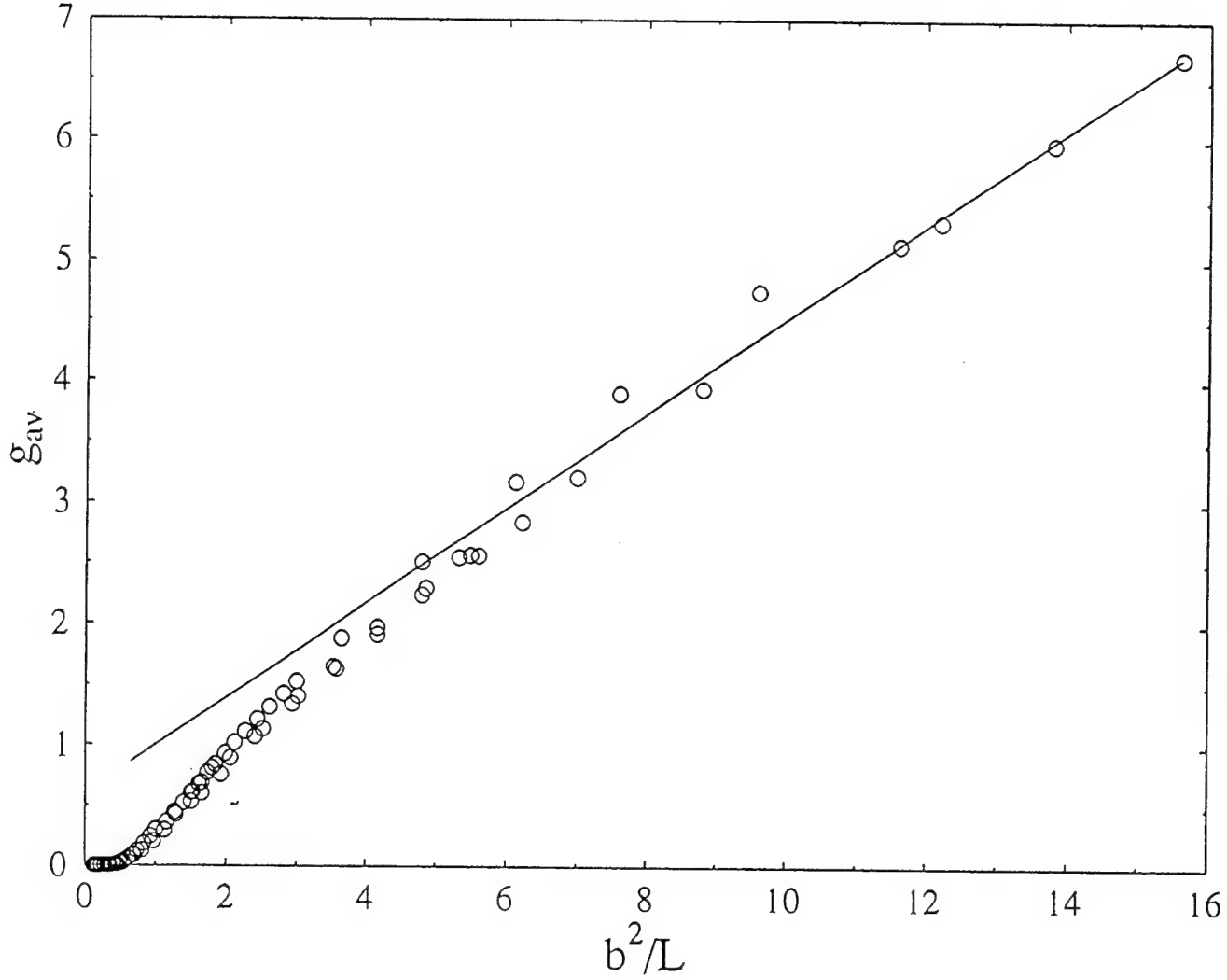

Fig. 3

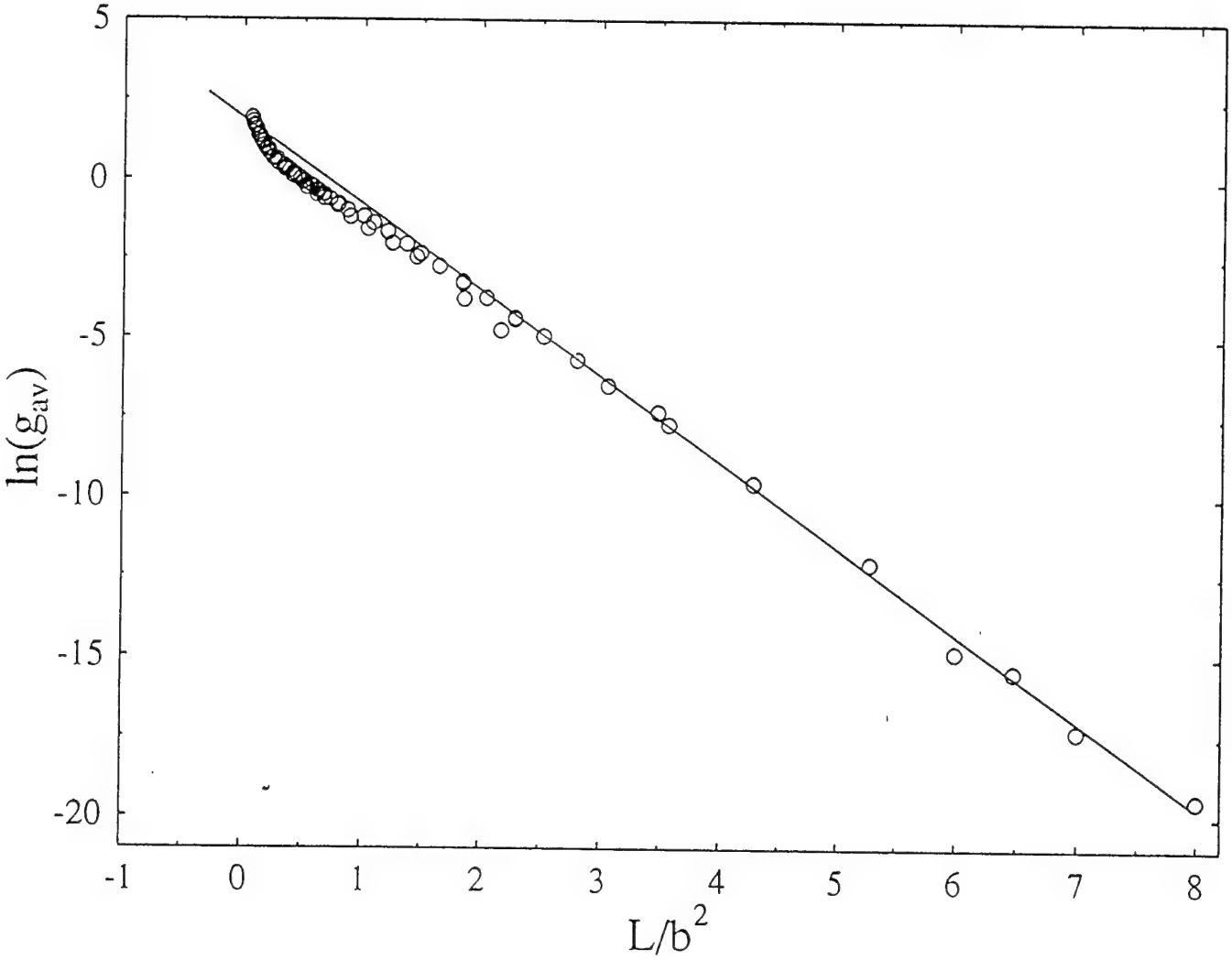

Fig. 4

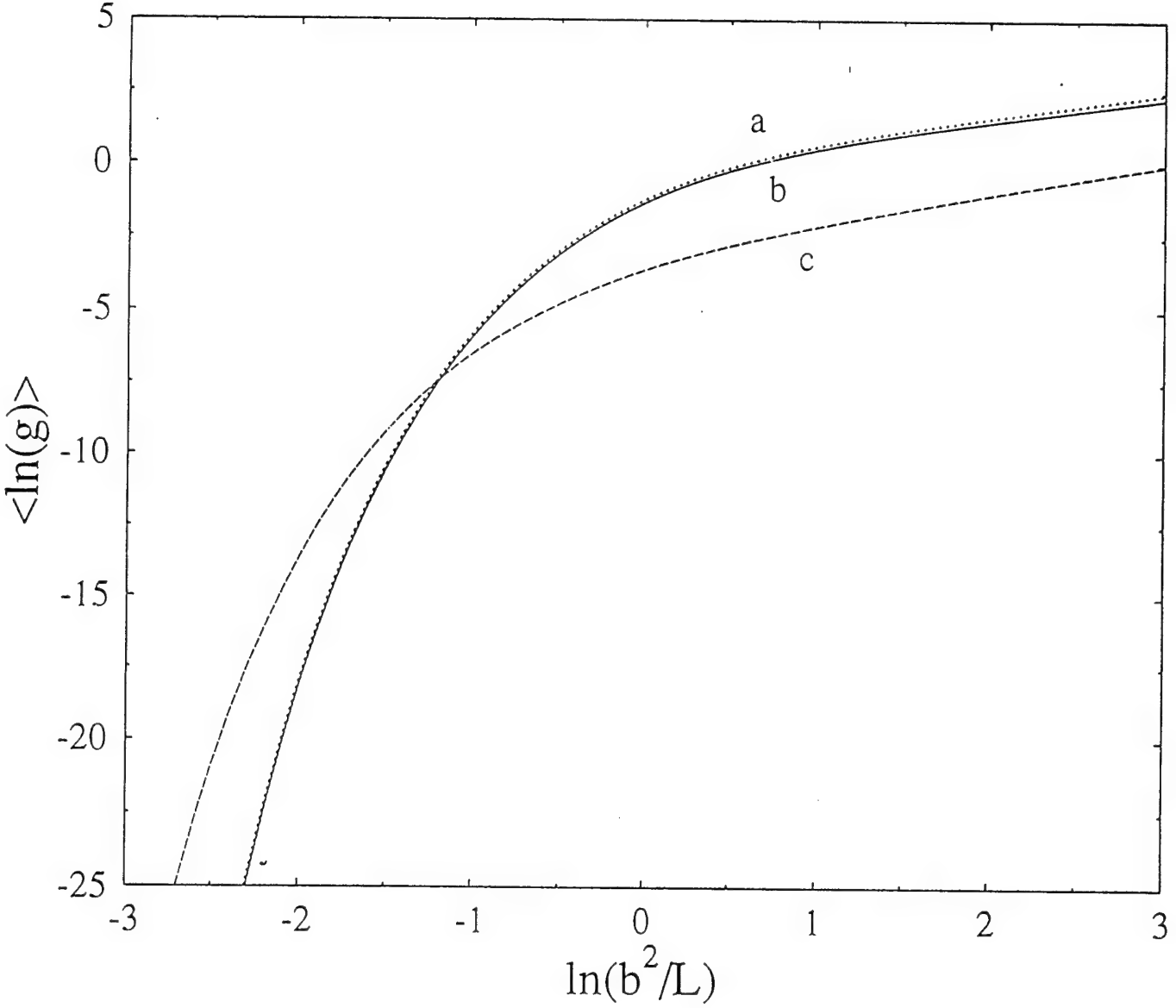

Fig. 5

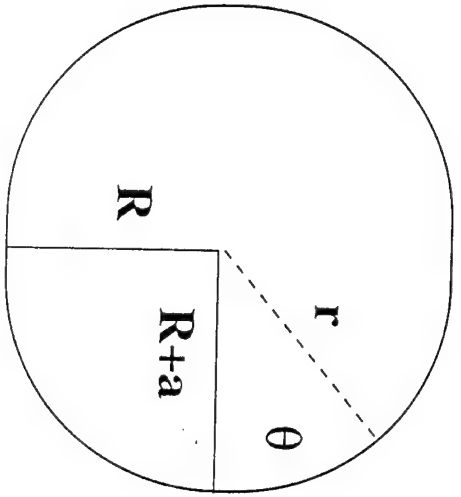

Fig. 6

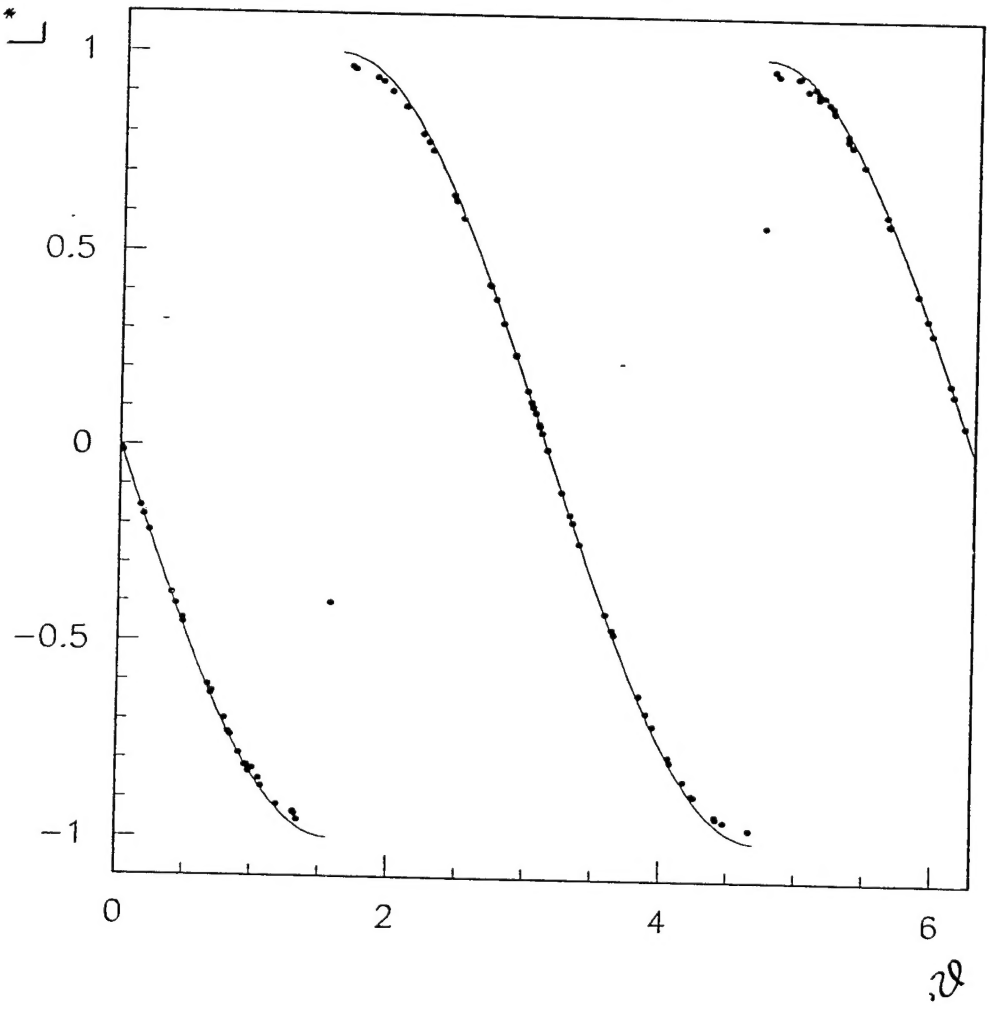

Fig. 7

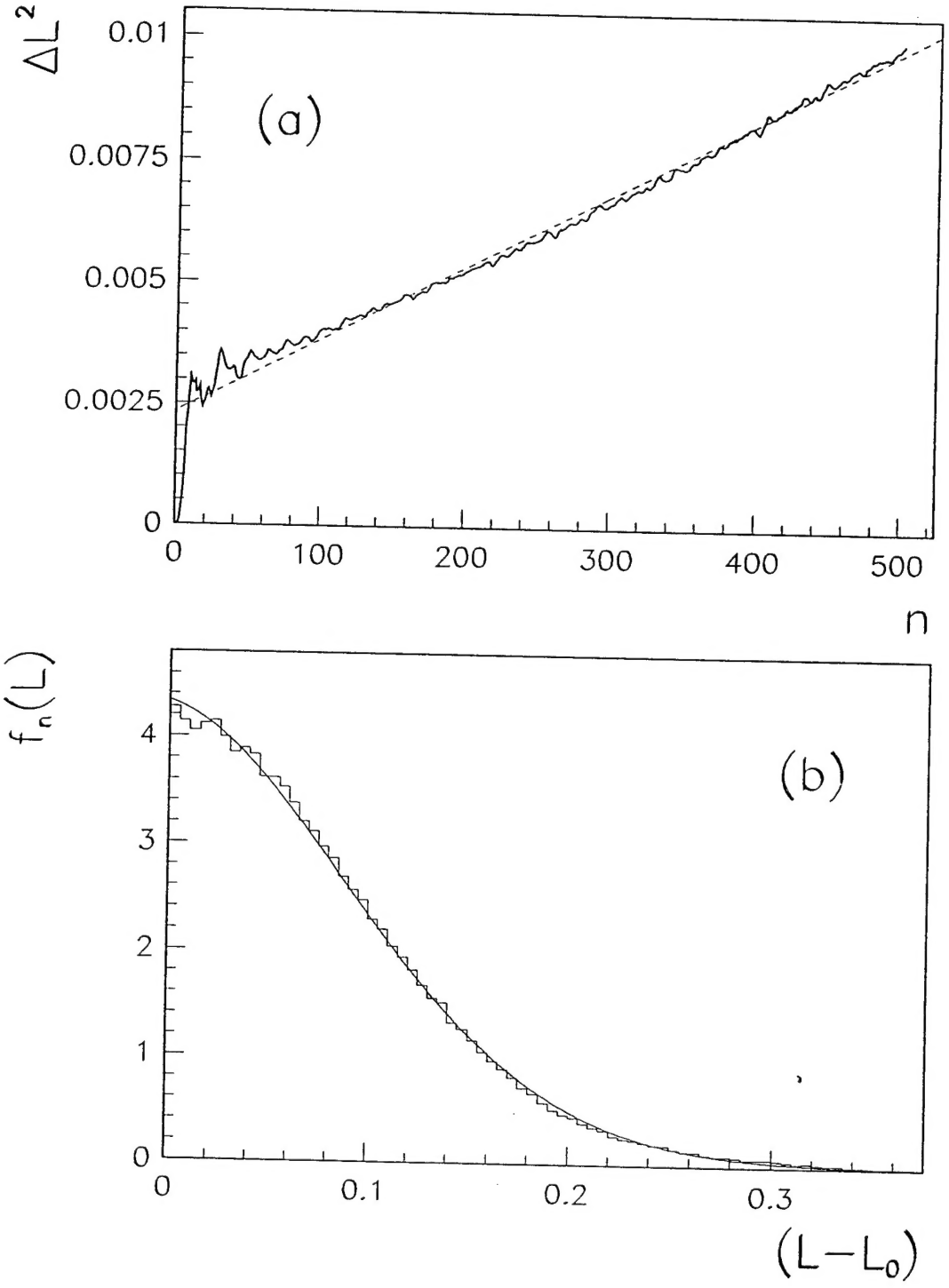
ΔL^2
0.01
0.0075
0.005
0.0025
0
(a)
0
100
200
300
400
500
n
$f_n(L)$
4
3
2
1
0
(b)
0
0.1
0.2
0.3
$(L-L_0)$

Fig. 8

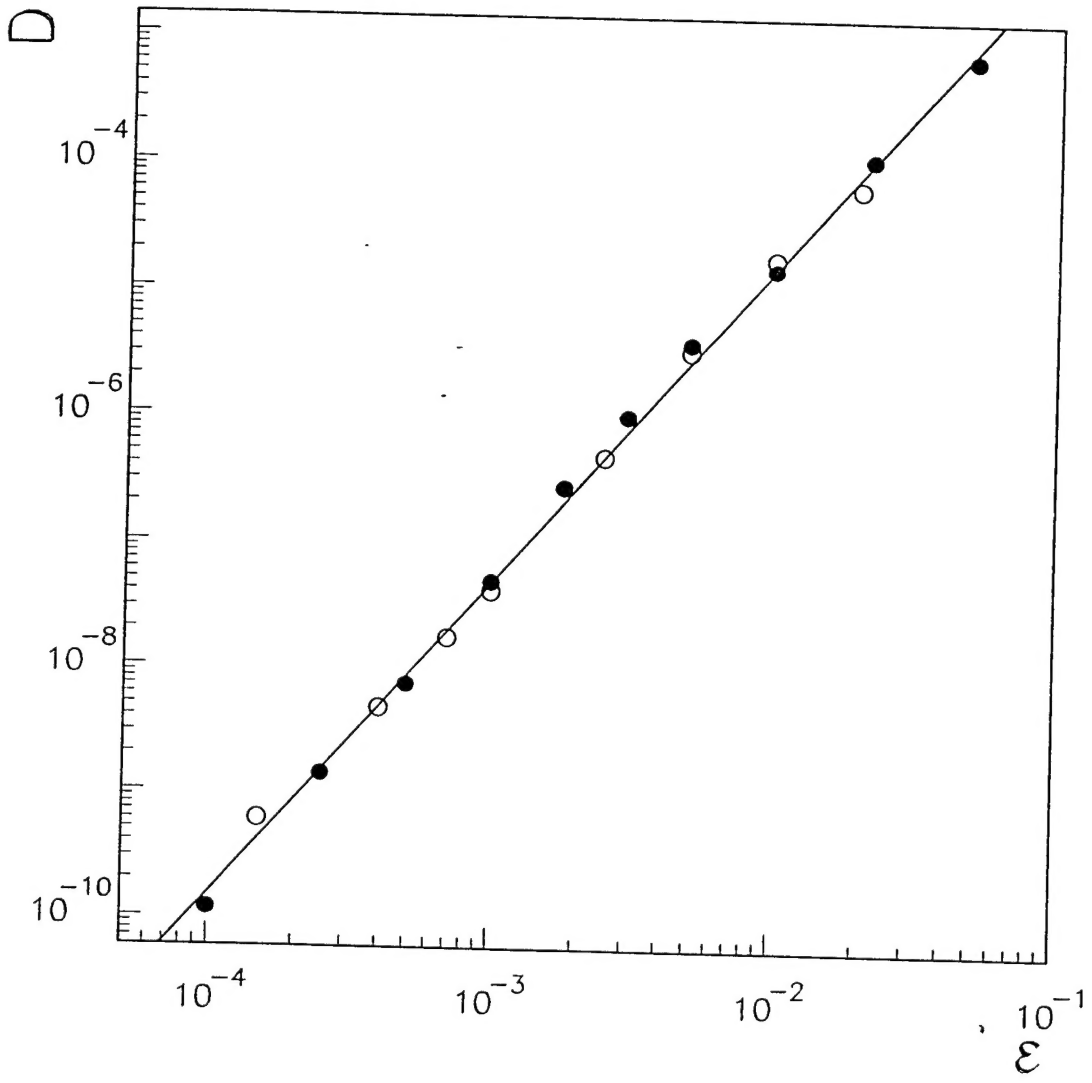

Fig. 9